

# Preparation and Processing of Molecular Composites of Rigid-Rod and Flexible-Chain Polymers from Soluble Complexes

Michael F. Roberts<sup>†</sup> and Samson A. Jenekhe\*

Department of Chemical Engineering and Center for Photoinduced Charge Transfer,  
University of Rochester, Rochester, New York 14627-0166

Received August 17, 1993. Revised Manuscript Received November 8, 1993\*

Molecular composites of rigid-rod poly(*p*-phenylene-2,6-benzobisthiazole) (PBZT) and flexible-chain polyamides, nylon 66 and poly((trimethylhexamethylene)terephthalamide) (PTMHT), have been prepared from ternary solutions of their coordination complexes in organic solvents and characterized. The measured ternary phase diagrams of the PBZT/polyamide/nitromethane-Lewis acid systems showed that the critical concentration for anisotropic phase appearance was as high as 8–10 wt %, depending on the rod/coil ratio and the Lewis acid (AlCl<sub>3</sub> or GaCl<sub>3</sub>) used. These critical concentrations are significantly higher than those attainable in similar ternary solutions of the polymers in protonic acid solvents. Films and coatings of PBZT/nylon 66 and PBZT/PTMHT molecular composites prepared from isotropic solutions were shown to be uniform with molecular level dispersion by various morphological characterization techniques. The favorable ternary solution phase equilibria and the processability from organic solvents make the present complexation mediated processing a promising approach for preparing polymer-based molecular composites for structural, optoelectronic, and photonic applications.

## Introduction

A molecular composite is a polymer blend in which a rigid-rod polymer is molecularly dispersed in the matrix of a flexible-chain polymer. Molecular composites have been of interest for more than a decade,<sup>1–20</sup> and the subject has been covered in recent symposia<sup>18</sup> and a review.<sup>19</sup> The

underlying concept is that molecular level reinforcement of a flexible-chain polymer with a rigid-rod polymer would yield a class of materials with superior mechanical properties, namely, vastly improved tensile strength and elastic modulus over the flexible-chain material and higher compressive strength and shear modulus than the pure rigid-rod polymer. However, a number of difficulties have been encountered in trying to develop molecular composites as viable practical materials. The fundamental problem arises from the thermodynamic incompatibility of rodlike and coillike polymers.<sup>21</sup> Rapid coagulation of isotropic solutions of the rod and coil polymers is therefore necessary to “freeze-in” the molecular dispersion of rodlike polymers in the flexible-chain polymer matrix. The lack of any alternative solvents to the strong protonic acids needed for processing of rigid-rod polymers such as poly(*p*-phenylene-2,6-benzobisthiazole) (PBZT) and poly(*p*-phenylene-2,6-benzobisoxazole) (PBO) is the root of many of the practical difficulties.<sup>19</sup> The low critical concentration ( $C_{cr} < 4$  wt %) for anisotropic phase appearance in PBZT solutions and in blend solutions of PBZT with flexible-chain polymers in methanesulfonic acid (MSA)<sup>3–10</sup> limits the processing of molecular composites since processing from anisotropic solutions inevitably leads to phase separated materials. Furthermore, the viscous nonvolatile nature of MSA can lead to phase separation during coagulation from isotropic solutions due to slow coagu-

<sup>†</sup> Current address: The Gillette Co., Boston Research & Development, One Gillette Park, Boston, MA 02127-1096.

\* To whom correspondence should be addressed.

• Abstract published in *Advance ACS Abstracts*, December 15, 1993.

(1) Helminiak, T. E. *ACS Div. Org. Coatings Plastic Chem. Prepr.* 1979, 40, 475.

(2) Takayanagi, M.; Ogata, T.; Morikawa, M.; Kai, T. *J. Macromol. Sci. Phys.* 1980, B17, 591–615.

(3) (a) Hwang, W.-F.; Wiff, D. R.; Verschoore, C.; Price, G. E.; Helminiak, T. E.; Adams, W. W. *Polym. Eng. Sci.* 1983, 23, 784–788. (b) Hwang, W.-F.; Wiff, D. R.; Verschoore, C. *Polym. Eng. Sci.* 1983, 23, 789–791.

(4) Hwang, W.-F.; Wiff, D. R.; Benner, C. L.; Helminiak, T. E. *J. Macromol. Sci. Phys.* 1983, B22, 231–257.

(5) Young, R. J.; Day, R. J.; Ang, P. P. *Polym. Commun.* 1990, 31, 47–49.

(6) Wang, C. S.; Goldfarb, I. J.; Helminiak, T. E. *Polymer* 1988, 29, 825–828.

(7) Chuah, H. H.; Kyu, T.; Helminiak, T. E. *Polymer* 1987, 28, 2130–2133.

(8) Kumar, S.; Wang, C. S. *Polym. Commun.* 1989, 29, 355–356.

(9) Crasto, A. S.; Gupte, K. M.; Lee, C. Y.-C. *Polym. Mater. Sci. Eng.* 1988, 59, 1101–1105.

(10) Hwang, C. R.; Malone, M. F.; Farris, R. J. *Polym. Mater. Sci. Eng.* 1988, 59, 440–444.

(11) Chuah, H. H.; Kyu, T.; Helminiak, T. E. *Polym. Mater. Sci. Eng.* 1988, 59, 1106–1110.

(12) Lee, C. Y.-C.; Swiatkiewicz, J.; Prasad, P. N.; Mehta, R.; Bai, S. *J. Polymer* 1991, 32, 1195–1199.

(13) Evers, R. C. In *Contemporary Topics in Polymer Science. Multiphase Macromolecular Systems*; Culbertson, B. M., Ed.; Plenum Press: New York, 1989; Vol. 6, pp 61–71.

(14) Krause, S. J.; Haddock, T. B.; Price, G. E.; Adams, W. W. *Polymer* 1988, 29, 195–206.

(15) Tsai, T. T.; Arnold, F. E.; Hwang, W.-F. *J. Polym. Sci. A, Polym. Chem.* 1989, 27, 2839–2848.

(16) Chuah, H. H.; Tan, L. S.; Arnold, F. E. *Polym. Eng. Sci.* 1989, 29, 107–112.

(17) Tan, L. S.; Arnold, F. E.; Chuah, H. H. *Polymer* 1991, 32, 1376–1379.

(18) (a) *The Materials Science and Engineering of Rigid-Rod Polymers. Mater. Res. Soc. Symp. Proc.* Adams, W. W., Eby, R. K., McLemore, D. E., Eds.; The Materials Research Society: Pittsburgh, 1989; Vol. 134, pp 507–585. (b) *Polymer Based Molecular Composites. Mater. Res. Soc. Symp. Proc.* Schaefer, D. W., Mark, J. E., Eds.; The Materials Research Society: Pittsburgh, 1990; Vol. 171.

(19) Wiff, D. R.; Helminiak, T. E.; Hwang, W.-F. In *High Modulus Polymers*; Zachariades, A. E., Porter, R. S., Eds.; Marcel Dekker: New York, 1988; pp 225–258.

(20) Hwang, W.-F.; Helminiak, T. E. *Mater. Res. Soc. Symp. Proc.* 1989, 134, 507–509.

(21) Flory, P. J. *Macromolecules* 1978, 11, 1138–1141.

lation rates. The thermodynamic incompatibility of rodlike and coillike polymer mixtures also leads to thermal instability of the molecular dispersion in molecular composites, so even if phase separation is avoided during coagulation, it may ensue during subsequent consolidation steps. Other problems such as degradation of the flexible-chain polymers in the acid solutions have also been encountered.<sup>16</sup>

Various experimental approaches have been explored in efforts to overcome the fundamental problem of preparing polymer molecular composites. Takayanagi et al.<sup>2</sup> prepared composites of polyarylamides with aliphatic polyamides in which the aromatic polyamide, poly(*p*-phenyleneterephthalamide) (PPTA), fibrils were 15–30 nm in diameter. They also prepared composites of nylon 66 with nylon 66/PPTA block copolymers. Good reinforcement of the nylon 66 matrix was achieved, but the fibril sizes indicated the lack of molecular level dispersion.<sup>2</sup> Hwang et al.<sup>3,4</sup> prepared composites of PBZT with flexible-chain analogs poly(benzothiazole) (ABPBT) and poly(benzimidazole) (ABPBI). Scanning electron microscopy (SEM) studies<sup>3b</sup> showed that there were no bulk features indicative of phase separation on a scale greater than 100 nm. Wide-angle X-ray diffraction experiments<sup>3b</sup> confirmed this and suggested that there may be PBZT crystallites of 30–40 nm size in the samples. Composite PBZT/ABPBT and PBZT/ABPBI materials with good mechanical properties were obtained (elastic moduli > 100 GPa)<sup>3–5</sup> and the intractable nature of both rod and coil components gave good thermal stability but also presented difficulties in consolidation into thicker samples. Aliphatic polyamides have also been employed as the flexible-chain components of molecular composites.<sup>6–12</sup> PBZT/zytel 42 composites were prepared by coagulation from MSA solutions by various schemes such as wet-spinning<sup>6–8</sup> and block coagulation<sup>9</sup> as well as an approach by Hwang and co-workers<sup>10</sup> in which a solution of zytel 42 in sulfuric acid was allowed to infiltrate PBZT fibers. However, phase separation in coagulated and thermally consolidated composites was encountered in all cases. PBZT rich domains of 2–7  $\mu\text{m}$  in size were seen in some coagulated materials<sup>7</sup> and phase separation kinetics were found to be rapid (minutes)<sup>11</sup> during the consolidation step, leading to grossly nonuniform materials. It was also suggested in a recent study<sup>12</sup> of the nonlinear optical properties of PBZT/zytel composites that unremovable residual MSA is present in these materials.

A number of synthetic approaches have also been attempted<sup>13–15</sup> in efforts to overcome the phase separation that destroys molecular dispersion. Rigid-rod polyimides have been generated in situ<sup>13</sup> in a compatible blend of two flexible-chain polymers, such as a polyisoimide and a polysulfone resin, one of which (the polyisoimide) is thermally isomerized to the requisite rigid-rod polymer in the final fabrication step. By this approach it was hoped that the problems of low  $C_{cr}$  can be overcome by processing from homogeneous blend solutions of the flexible-chain polymers at high concentration and that phase separation in the resulting composites will be minimized because the rigid-rod material is generated only as a final step in the processing. Unfortunately, polymer insolubility and phase separation were encountered in the systems studied. Krause et al.<sup>14</sup> among others<sup>15</sup> have investigated triblock ABA copolymers of ABPBI (A) and PBZT (B). They rationalized that chemical bonding of the rod and coil

polymers would lead to a retardation of phase separation both in solution and in solid composites. Some improvements in  $C_{cr}$  and mechanical properties were obtained, and it was claimed from transmission electron microscopy (TEM) studies that samples were uniform to a level of 3 nm. In a similar vein, graft copolymers of polybenzimidazole with flexible side chains have also been prepared<sup>15</sup> with the aim of improving  $C_{cr}$  and polymer solubility. Yet another approach to the problem has been attempted by Chuah et al.,<sup>16</sup> who tried to use bisbenzocyclobutene oligomers as a thermosetting matrix host for PBZT. However, severe degradation of the coil polymer was observed in MSA solutions. Also, the composites phase separated during coagulation because of insufficient entanglement of the rod molecules by the low molecular weight flexible-chain molecules.<sup>16</sup> The same authors have also recently proposed<sup>17</sup> to make molecular composites of PBZT with a polysulfonate in the hope of retarding phase separation in the final products by inducing ionic interactions between the rod and coil polymers.

In light of all these studies and the problems encountered,<sup>1–20</sup> the barriers to the realization of a true molecular composites technology can, in our view, be summarized as follows: there is clearly a need for a solution processing route that overcomes the problems associated with processing from protonic acids such as MSA. Solvent systems that can cosolubilize the rigid-rod and flexible-chain polymers without degradation of either are needed. High critical concentrations are necessary to allow preparation of molecular composites from a wider range of solution concentrations. Coagulation media and nonsolvent systems are required which allow facile complete solvent removal and rapid coagulation to prevent phase separation. In addition, polymer composite systems are required which avoid the problems of phase separation during consolidation. To this end, one can envisage at least two possible scenarios: (a) a solvent system from which molecular composites can be coagulated in the desired final form, without the need for further consolidation, or (b) rod/coil polymer pairs in which phase separation is sufficiently retarded, by intermolecular interactions or other means, to prevent its occurrence during sample consolidation.

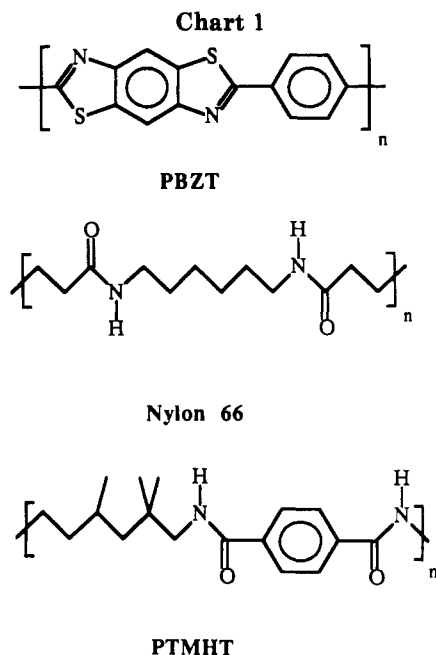
In this paper we report the method of complexation-mediated processing of molecular composites of rigid-rod and flexible-chain polymers. By using this approach, we have been able to overcome many of the difficulties of preparing molecular composites, discussed above. In a recent communication,<sup>22</sup> we reported the feasibility of using this technique to produce thin films of molecular composites of the rigid-rod polymer PBZT with each of the flexible chain polymers nylon 66 and poly((trimethylhexamethylene)terephthalamide) (PTMHT) for study of third-order nonlinear optical properties. The proposed method involves cosolubilization of the component polymers in organic solvents by means of a reversible coordination complexation of the polymers with metal halide Lewis acids. We have previously reported on the soluble complexes of rigid-rod and flexible-chain polymers.<sup>23–26</sup>

(22) Roberts, M. F.; Jenekhe, S. A. *Chem. Mater.* **1990**, *2*, 629–631.

(23) (a) Jenekhe, S. A.; Johnson, P. O.; Agrawal, A. K. *Macromolecules* **1989**, *22*, 3216–3222. (b) Jenekhe, S. A.; Johnson, P. O. *Macromolecules* **1990**, *23*, 4419–4429.

(24) (a) Roberts, M. F.; Jenekhe, S. A. *Polym. Commun.* **1990**, *31*, 215–217. (b) Roberts, M. F.; Jenekhe, S. A. *Chem. Mater.*, in press.

(25) Roberts, M. F.; Jenekhe, S. A. *Chem. Mater.* **1990**, *2*, 224–226.



Here we examine the solution-phase equilibria of blend solutions of various compositions of rigid-rod PBZT with flexible-chain nylon 66 and PTMHT (Chart I), and two different Lewis acids ( $\text{AlCl}_3$  and  $\text{GaCl}_3$ ) in aprotic organic solvents. The composition, structure and morphology of rod-coil molecular composites coagulated from isotropic solutions are characterized over a range of rod:coil ratios.

Although the primary reason for the wide interest in polymer molecular composites is because of their potential as structural materials,<sup>1-20</sup> our interests in preparing molecular composites come primarily from our belief that they are excellent model systems for studying the effects of composition, structure, and morphology on the electronic, optoelectronic, and nonlinear optical properties of organic materials and as such they are a useful means to tailor and enhance these properties. Our initial studies of these aspects of molecular composites are presented elsewhere.<sup>27</sup>

### Experimental Section

The PBZT sample was provided by the Polymer Branch of the Air Force Materials Laboratory, Dayton, OH. The sample had an intrinsic viscosity  $[\eta]$  of 18 dL/g in MSA at 30 °C. Nylon 66 of  $M_w$  12 000–18 000 ( $[\eta] = 0.99$  dL/g in *m*-cresol at 40 °C) has a glass transition temperature ( $T_g$ ) of 55 °C and a crystalline melting point of 260 °C. This sample was obtained from Polysciences Inc. Warrington PA. PTMHT ( $[\eta] = 0.94$  dL/g in *m*-cresol at 40 °C) with a  $T_g$  of 153 °C was obtained from Scientific Polymer Products, Ontario, NY. Nitromethane (NM) (99+%), gallium(III) chloride (99.99+%), and aluminum(III) chloride (99.99%) were purchased from Aldrich and used without further purification.

All polymer solutions were prepared in a Vacuum Atmospheres drybox filled with nitrogen, as follows: Predetermined amounts of polymer were weighed and added to solutions of known concentrations of Lewis acid ( $\text{AlCl}_3$  or  $\text{GaCl}_3$ ) in nitromethane. Sufficient Lewis acid was provided in solution in each case to form the soluble coordination complexes of the various polymers.<sup>22-26</sup> This means at least 1 mol of Lewis acid/mol of the N

and S heteroatoms in PBZT, and the carbonyl oxygens in the polyamides (see Chart I). Polymer dissolution was aided by mechanical stirring and/or gentle heating at 40–60 °C. These solutions were allowed to stand for several days to allow the polymers to completely dissolve and to allow for phase equilibration of the resulting solutions.

The optical anisotropy of ternary solutions was measured as a function of polymer concentration in order to establish the ternary phase diagrams. Solution anisotropy was detected by observation of the appearance of a mesophase in solution aliquots pressed between microscope coverslips by using polarized light optical microscopy. A series of solutions of each rod/coil pair (PBZT/nylon 66 and PBZT/PTMHT) at different ratios (1:2, 1:1, and 2:1 moles of repeat units) and different solvent media ( $\text{AlCl}_3/\text{NM}$  and  $\text{GaCl}_3/\text{NM}$ ) was prepared, of varying total polymer concentration. The critical concentrations were then measured as the highest polymer concentration, in each ternary rod/coil/solvent system, which did not exhibit a mesophase.

Lewis acid complexes of the rod/coil molecular composites were isolated from their solutions by slow evaporation of the solvent. Typically, the complexes were dried at 80–100 °C by placing a weighed amount of solution on a glass substrate onto a controlled surface temperature (80–100 °C) hot plate in the drybox for 8–10 h. All complexes were handled under nitrogen or vacuum until coagulation because of the likelihood of moisture contamination under atmospheric conditions.

Coagulation of composites was accomplished by either of two means: (1) The Lewis acid complex of the composite, prepared as described above, was immersed in deionized water or methanol to remove the Lewis acid or (2) aliquots of solution were immersed in deionized water or methanol for 12–16 h in order to remove the Lewis acid and solvent. The coagulates obtained were dried in vacuum at 60–80 °C for 12–24 h. Water and methanol are suitable coagulation solvents because of their high donor numbers which cause them to decompose and so precipitate the polymers.<sup>23</sup>

Thermal analysis was done by using duPont Model 2100 thermal analyst based on an IBM PS/2 Model 60 computer and equipped with a Model 910 differential scanning calorimeter (DSC) and a Model 951 thermogravimetric analyzer (TGA). All thermal analysis was done with the samples under a nitrogen purge using heating rates of 20 and 10 °C/min for DSC and TGA runs, respectively. DSC scans were calibrated by using an indium (mp = 156.6 °C) standard. DSC samples of composites were coded to room temperature in air and then further cooled to –25 °C with dry ice/acetone between runs.

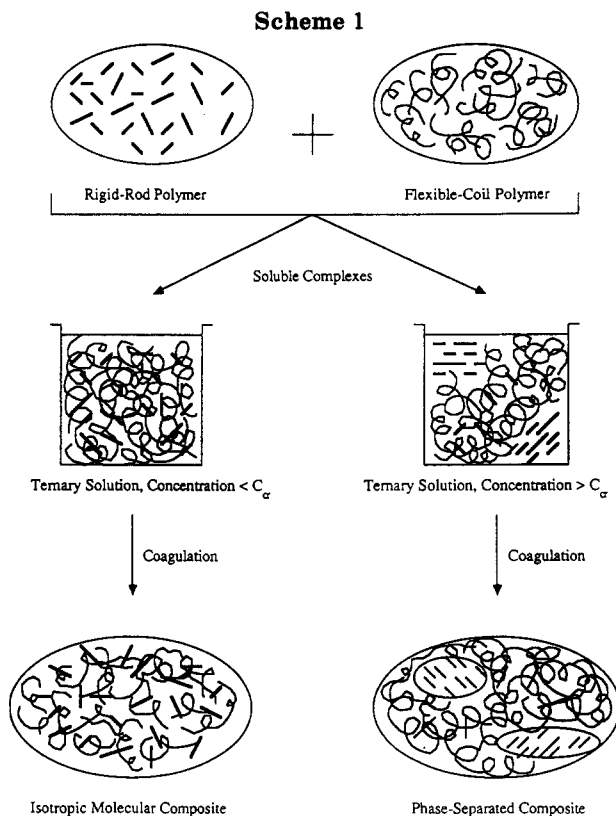
All optical microscopy (OM) was done by using an Olympus Model BH2 polarizing microscope. Samples of the molecular composites for OM were solution cast thin films (> 1  $\mu\text{m}$ ) on glass microscope slides. Scanning electron microscopy (SEM) was done by using a Cambridge Stereoscan Model 200 microscope. Films of the molecular composites for SEM were coated with 50–100 Å of gold prior to examination. Samples for X-ray diffraction were flat films 3–5  $\mu\text{m}$  thick. X-ray powder diffraction patterns were obtained for us by Oneida Research Services (Whitesboro, NY) with a Siemens D500 diffractometer equipped with a graphite monochromator. The instrument was set up with a  $\text{Cu K}\alpha$  radiation X-ray source operating at 50 kV and 40 mA. The  $2\theta$  scan range was set to 4–80° by using a step scan window of 0.05°/1.0 s step. Calibration was performed with an NBS mica standard (SRM 675). Data were collected and reduced with the use of a Micro VAX II computer. Fourier transform infrared (FTIR) spectra of the coagulated composites were collected on a Nicolet Model 20SXC spectrometer. Samples for FTIR analysis were free-standing thin films supported on steel wire frames. UV-visible spectroscopy of thin films (< 0.5  $\mu\text{m}$ ) of composites coated on fused silica substrates was carried out on a Perkin-Elmer Lambda 9 spectrophotometer.

### Results and Discussion

The overall procedure for the complexation-mediated preparation of molecular composites is shown in Scheme 1. The rigid-rod polymer (PBZT) and flexible-coil polymer (nylon 66 or PTMHT) are codissolved in an aprotic organic solvent (nitromethane) via their Lewis acid ( $\text{AlCl}_3$  or  $\text{GaCl}_3$ )

(26) Roberts, M. F.; Jenekhe, S. A. *Macromolecules* 1991, 24, 3142–3146.

(27) (a) Vanherzeele, H.; Meth, J. S.; Jenekhe, S. A.; Roberts, M. F. *Appl. Phys. Lett.* 1991, 58, 663–665. (b) Vanherzeele, H.; Meth, J. S.; Jenekhe, S. A.; Roberts, M. F. *J. Opt. Soc. Am. B* 1992, 9, 524–533.



coordination complexes.<sup>22–26</sup> Molecular composites can only be processed from ternary solutions of the component polymer complexes which are isotropic. For a given rod:coil polymer ratio there is a maximum total polymer concentration in solution ( $C_{cr}$ ) above which the rigid-rod polymer will phase separate into a liquid-crystalline phase. Composite coagulation from anisotropic solutions (concentration  $> C_{cr}$ ) inevitably leads to phase-separated materials since molecular dispersion of the polymers has already been destroyed in solution. In the following we first discuss the solution-phase equilibria of the PBZT/nylon 66 and PBZT/PTMHT systems in Lewis acid/nitromethane and then our characterization and study of the molecular composites prepared.

**Phase Equilibria in Solution.** The solutions of complexes of rigid-rod/flexible-coil polymers in Lewis acid/nitromethane are, strictly speaking, quaternary systems: (1) rigid-rod polymer, (2) flexible-coil polymer, (3) Lewis acid, (4) organic solvent. However, they can be regarded as ternary systems if the Lewis acid and organic solvent are collectively taken as solvent. The critical concentrations for PBZT/nylon 66 and PBZT/PTMHT systems complexed with each of the Lewis acids  $\text{AlCl}_3$  and  $\text{GaCl}_3$  in nitromethane are tabulated in Table 1 and the corresponding ternary phase diagrams are shown in Figures 1 and 2. The typical critical concentration of PBZT in MSA has been found to be less than 4 wt %.<sup>4</sup> The data in Table 1 show values in  $\text{AlCl}_3/\text{NM}$  to be significantly higher and in the case of  $\text{GaCl}_3/\text{NM}$  solutions  $C_{cr}$  values of the order of 2 times the MSA values are seen. Solution isotropy can therefore be maintained to much higher polymer concentrations and so molecular composites can be processed at higher concentrations from Lewis acid/nitromethane solutions than from MSA or other protonic acids.

One of the most important results in Table 1 and Figures 1 and 2 is the dramatic effect of Lewis acid variation ( $\text{AlCl}_3$

**Table 1. Critical Concentrations ( $C_{cr}$ , wt %) for Anisotropic Phase Separation in Ternary Solutions of PBZT/Polyamide/Lewis Acid–Nitromethane**

PBZT: nylon 66 <sup>a</sup>	$C_{cr}$		PBZT: PTMHT <sup>a</sup>	$C_{cr}$	
	$\text{AlCl}_3/\text{NM}^b$	$\text{GaCl}_3/\text{NM}^c$		$\text{AlCl}_3/\text{NM}^b$	$\text{GaCl}_3/\text{NM}^c$
1:0	5.0	8.0	1:0	5.0	8.0
2:1	5.0	8.5	2:1	5.3	8.5
1:1	5.1	9.0	1:1	5.7	9.5
1:2	5.4	10.0	1:2	6.3	10.5

<sup>a</sup> Mole ratio of polymer repeat units. <sup>b</sup> Accuracy is  $\pm 0.2$  wt %.  
<sup>c</sup> Accuracy is  $\pm 0.3$  wt %.

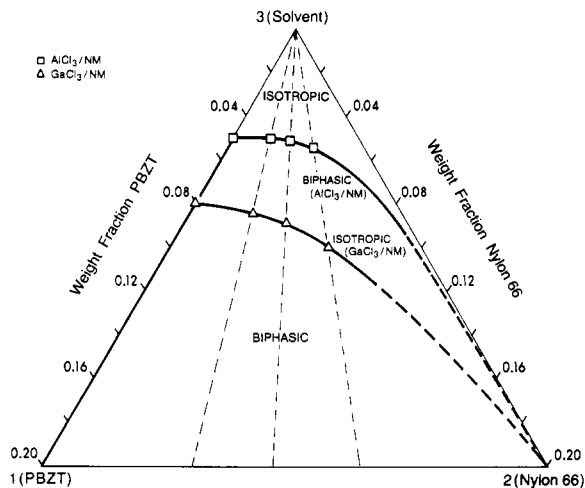


**Figure 1.** Ternary phase diagrams of PBZT/nylon 66 in  $\text{AlCl}_3/\text{NM}$  ( $\square$ ) and in  $\text{GaCl}_3/\text{NM}$  ( $\triangle$ ).

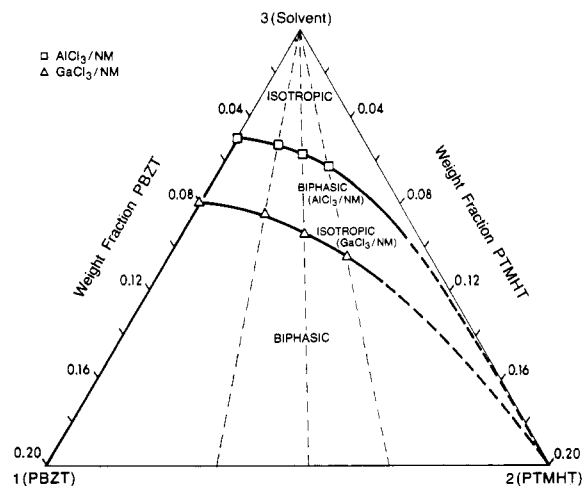


**Figure 2.** Ternary phase diagrams of PBZT/PTMHT in  $\text{AlCl}_3/\text{NM}$  ( $\square$ ) and in  $\text{GaCl}_3/\text{NM}$  ( $\triangle$ ).

or  $\text{GaCl}_3$ ) on the phase equilibria of PBZT/polyamide/solvent systems. It is seen that by going from  $\text{AlCl}_3$  to  $\text{GaCl}_3$  the critical concentration is increased by 60–85% depending on the rod:coil ratio. One implication of this result is that other Lewis acids may further increase  $C_{cr}$  values and hence enlarge the isotropy regions of the phase diagrams essential to preparing rod/coil polymer molecular composites. In any case, this variability and control of the ternary phase equilibria of rod/coil/solvent systems by varying the solvent composition is unique to the complexation mediated processing approach to molecular composites.

The data of Table 1 and Figures 1 and 2 indicate that the critical concentration  $C_{cr}$  is not very sensitive to the nature of the coil polymer. Thus the  $C_{cr}$  values of PBZT/

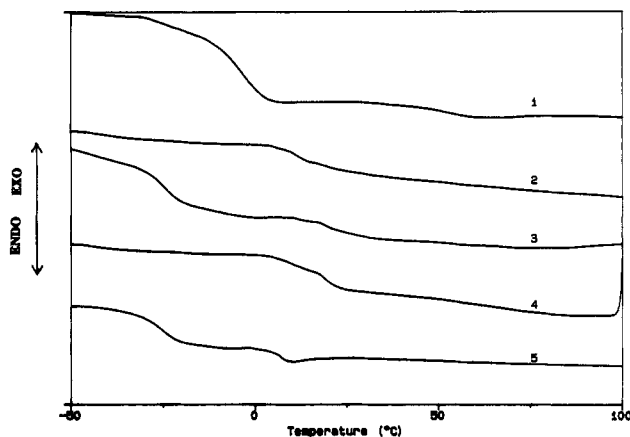


**Figure 3.** DSC thermograms of  $\text{GaCl}_3$  complexes of (1) nylon 66, (2) PBZT, (3) 2:1 PBZT:nylon 66, (4) 1:1 PBZT:nylon 66, and (5) 1:2 PBZT:nylon 66. Heating rate: 20 °C/min.

nylon 66 are nearly identical to those of PBZT/PTMHT in the two different organic solvents ( $\text{AlCl}_3/\text{NM}$  and  $\text{GaCl}_3/\text{NM}$ ). This may seem surprising considering the difference in chain flexibility between nylon 66 and PTMHT. The phase equilibria of other PBZT/flexible-coil polymer/nitromethane-Lewis acid systems are expected to be similar to PBZT/nylon 66 and PBZT/PTMHT and hence the present data can be used to estimate the  $C_{cr}$  values of other molecular composite systems containing new flexible-coil polymers.

The trends of  $C_{cr}$  in Table 1 and Figures 1 and 2 are in good agreement with Flory's theoretical predictions.<sup>21</sup> Firstly,  $C_{cr}$  increases monotonically as the coil:rod ratio increases. Also, as the coil:rod ratio increases, the fraction of PBZT in solution at  $C_{cr}$  decreases. In the extreme case of pure coil polymer (nylon 66 or PTMHT) solutions, anisotropic phase separation is never observed. A quantitative comparison of the experimental data for the PBZT/nylon 66 solutions with the theory by using axial ratios  $X_1$  and  $X_2$  of 275 and 265 for PBZT and nylon 66, respectively, yielded a binodal curve which lies well above those in Figure 1 (i.e., lower  $C_{cr}$ ). These axial ratios were calculated for the pure polymers by Flory's method<sup>28</sup> by using the respective PBZT and nylon 66 repeat unit lengths of 12.5<sup>29</sup> and 17.4 Å<sup>30</sup> and densities of 1.44<sup>29</sup> and 1.14 g/cm<sup>3</sup>.<sup>31</sup> The molecular weights of PBZT and nylon 66 used in the calculation were 29 500 and 15 000, respectively. Considering the structures of the Lewis acid complexes, it is reasonable that the coordinated Lewis acids may act as attached side groups and thereby lower the axial ratios of the polymers. Good fits to the experimental data were obtained by using axial ratios of 98 for the  $\text{GaCl}_3$  complex of PBZT and 141 for the  $\text{AlCl}_3$  complex. Axial ratios of the nylon 66 complexes, which do not have much effect on the overall results were, for simplicity, scaled down by similar factors giving  $X_2 = 93$  and 137, respectively, for the  $\text{GaCl}_3$  and  $\text{AlCl}_3$  complexes. Given the approximations of the theory, such as its neglect of enthalpic effects, we have nonetheless a good explanation of the origin of the higher critical concentrations of the polymer complexes

in organic solvents, compared with the pure polymers in MSA solutions. That is, by complexing the polymers with Lewis acids one effectively lowers the axial ratios and thereby increases critical concentrations.

The solid-state  $\text{GaCl}_3$  complexes of PBZT/PTMHT and PBZT/nylon 66 were malleable and ductile at room temperature. We have previously observed similar phenomena for the component polymer complexes and attributed this to the low  $T_g$ 's exhibited by the complexes.<sup>25,32</sup> Figure 3 shows DSC scans of the complexes of nylon 66, PBZT, and their composites. Curves 1 and 2 show  $T_g$  transitions of nylon 66 and PBZT complexes at -5 and 26 °C, respectively. The overlap of these separate  $T_g$ 's can be seen in curve 4. In the PBZT/nylon 66 complex of curve 4, only sufficient  $\text{GaCl}_3$  was used to coordinate each of the four heteroatoms (two N and two S atoms) of PBZT and each carbonyl oxygen of nylon 66. The PBZT/nylon 66 complexes of curves 3 and 5 contained large excesses (~50%) of the Lewis acid over this amount which is the minimum necessary for solubilization of the polymers.<sup>23-25</sup> The effect of these large excesses of Lewis acid is to separate the overlapping  $T_g$ 's of the rod and coil polymer complexes. In curve 3 two glass transitions are evident, one at -25 °C and the other at about 20 °C. In curve 5, two transitions are also evident at -25 and 7 °C. The separate  $T_g$ 's in curves 3 and 5, and the overlapping  $T_g$ 's in curve 4 indicate that the PBZT/nylon 66 complexes are phase-separated materials. This is just what is predicted by lattice theory,<sup>21</sup> i.e., that in the limiting case of concentrated solutions, the rod and coil molecules are thermodynamically incompatible. The low  $T_g$ 's of the complexes result in phase separation at ambient temperatures.

**Coagulation and Characterization of Molecular Composites.** Molecular composites of PBZT/nylon 66 and PBZT/PTMHT over a broad range of composition (rod:coil ratio) were coagulated from isotropic solutions. We chose to study composites of composition corresponding to 2:1, 1:1 and 1:2 mole ratios of rod:coil repeating units or 70/30, 54/46, and 37/63 wt % PBZT/nylon 66 and 66/34, 48/52, and 32/68 wt % PBZT/PTMHT. Data were also collected for the pure polymers thus giving coverage of the full composition range.

**Thermal Analysis.** Figure 4 shows thermogravimetric analysis (TGA) curves for component polymers and their molecular composites coagulated from isotropic solutions in  $\text{AlCl}_3/\text{NM}$ . Exactly superimposable curves were obtained from composites coagulated from  $\text{GaCl}_3/\text{NM}$ . The TGA data for the composites clearly show features of the decomposition of the rigid-rod and the flexible-chain polymers, namely, the onset of weight loss near 400, 430, and 720 °C indicates nylon 66, PTMHT, and PBZT, respectively. From the percentage weight loss of each pure polymer by a certain temperature (600 °C for nylon 66 and PTMHT and 900 °C for PBZT) we calculated the composition of each composite from their TGA curves. These results are also shown in Figure 4. For the PBZT:nylon 66 molecular composites these weight ratios are within ~2 wt % of the mole ratios 2:1, 1:1, and 1:2 of repeat units dissolved in the original solutions. The measured compositions of PBZT:PTMHT were similarly

(28) Flory, P. J. *Adv. Polym. Sci.* 1984, 59, 1-35.

(29) Wellman, M. W.; Adams, W. W.; Wolff, R. A.; Dudis, D. S.; Wiff, D. R.; Fratini, A. V. *Macromolecules* 1981, 14, 935-939.

(30) Baker, W. O.; Fuller, C. S. *J. Am. Chem. Soc.* 1942, 64, 2399-2407.

(31) Zimmerman, J. *Encyclopedia of Polymer Science and Engineering*, 2nd ed.; Wiley: New York, 1988; Vol. 11, pp 315-381.

(32) (a) Roberts, M. F.; Jenekhe, S. A. *Mater. Res. Soc. Symp. Proc.* 1991, 215, 23-28. (b) Jenekhe, S. A.; Roberts, M. F. *Macromolecules* 1993, 26, 4981-4983.

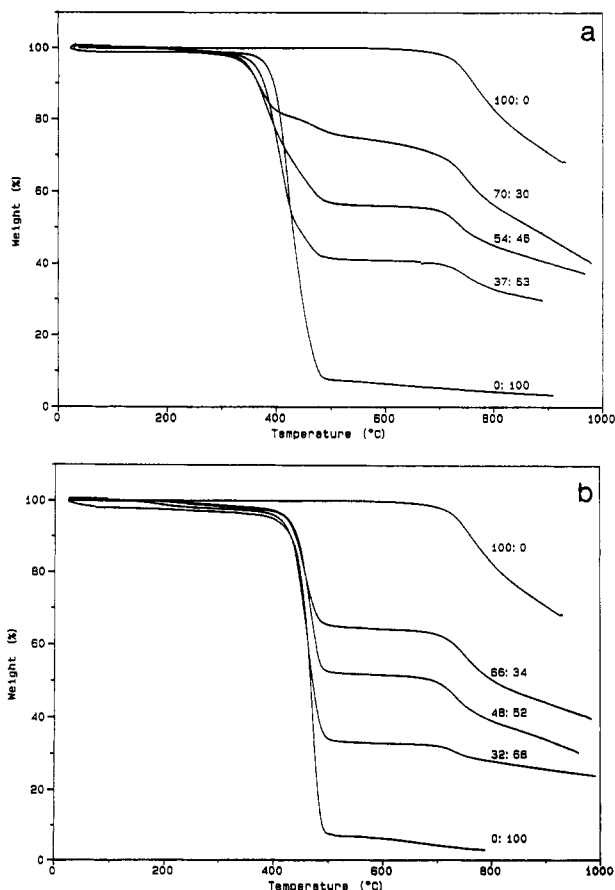


**Figure 4.** TGA weight loss curves of (a) PBZT/nylon 66 and (b) PBZT/PTMHT molecular composites. Ratios in this figure are weight ratios of PBZT:polyamide.

close to the mole ratios of repeat units of 2:1, 1:1, and 1:2, respectively.

Figure 5 shows successive DSC scans on samples of PBZT/PTMHT composites coagulated from isotropic  $\text{AlCl}_3/\text{NM}$  solutions. In Figure 5a a broad endotherm shows up in the first scan of the 2:1 composite with a peak near  $80^\circ\text{C}$  and the  $T_g$  of PTMHT at  $153^\circ\text{C}$  is absent. This  $T_g$  gradually reappears in the second scan and is very clearly in evidence in run 3. In the 1:1 PBZT:PTMHT molecular composite a broad endotherm peaking near  $110^\circ\text{C}$  is again visible on the first DSC run in Figure 5b. The  $T_g$  of PTMHT is seen to gradually reappear during the second and third scans. Figure 5c shows that the broad endotherm has shifted to an even higher temperature in the initial scans of the 1:2 composite, this time peaking around  $180^\circ\text{C}$  and consequently enveloping the glass transition region of PTMHT. As in the other cases the  $T_g$  of PTMHT shows up clearly in subsequent scans.

The fact that the  $T_g$  of PTMHT is absent in the initial scans of the composites is evidence of the molecular dispersion in the as-processed materials. Since PBZT shows no clear  $T_g$  of its own, a "composite"  $T_g$  intermediate between the rod and coil polymer  $T_g$ 's does not appear. However the gradual reappearance of the glass transition of PTMHT in subsequent DSC scans in each case does indicate thermally induced phase separation, whereby regions rich in amorphous PTMHT are formed. We believe that the endotherms seen in the initial DSC scans are characteristic of this phase separation. The absence of any solvent or other volatile impurities in the as-processed materials is shown clearly in the TGA data of

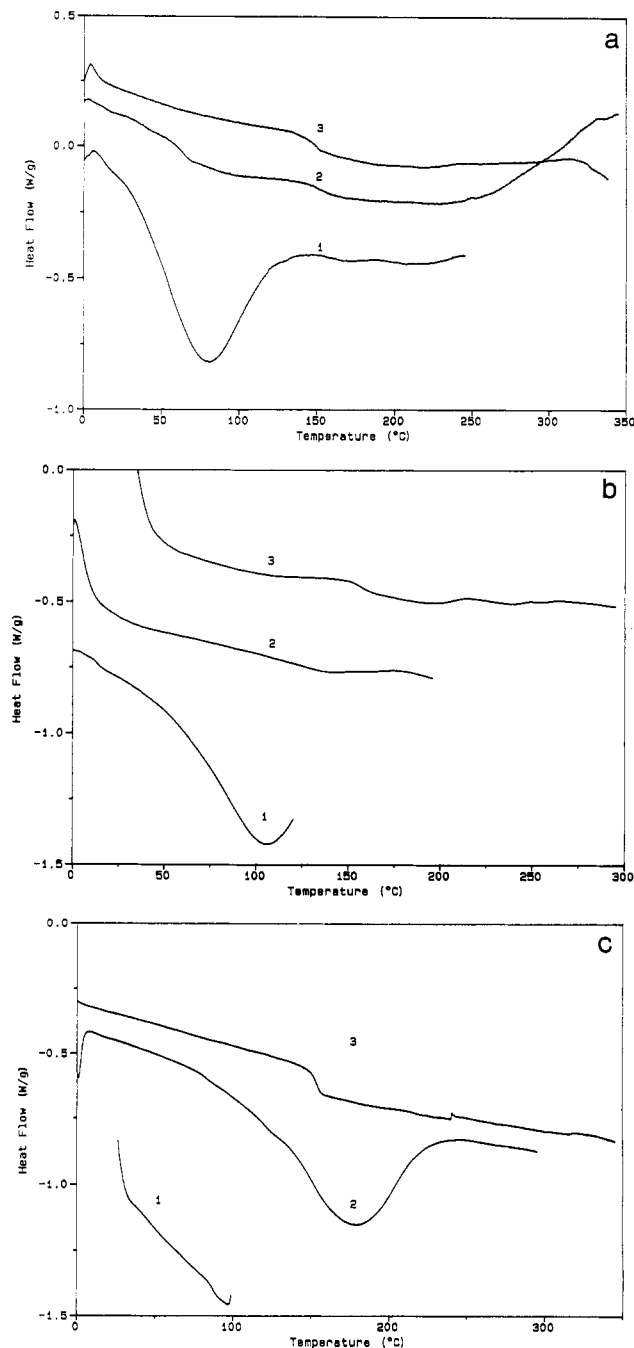


**Figure 5.** DSC thermograms of PBZT:PTMHT molecular composites (a) 2:1, (b) 1:1, (c) 1:2. The curve numbers indicate the chronological order of DSC scans. Heating rate:  $20^\circ\text{C}/\text{min}$ .

Figure 4, and so we must conclude that the endotherms arise from internal rearrangements of the composite morphologies. The appearance of the coil polymer  $T_g$  indicates that this process is phase separation. The shift of this endotherm to higher temperature with increasing PTMHT content suggests an increasing stability to phase separation. This means that the composites of higher PBZT content undergo phase separation at lower temperatures than those of lower rod content.

Figure 6 shows the results of similar DSC experiments on PBZT/nylon 66 molecular composites. Broad endotherms are seen with peak temperatures of  $85$ ,  $125$ , and  $160^\circ\text{C}$  in the initial DSC scans of 2:1, 1:1, and 1:2 PBZT:nylon 66 respectively. This indicates thermally induced phase separation in the samples, as seen in the PBZT/PTMHT case, and again the trend of increasing peak temperature

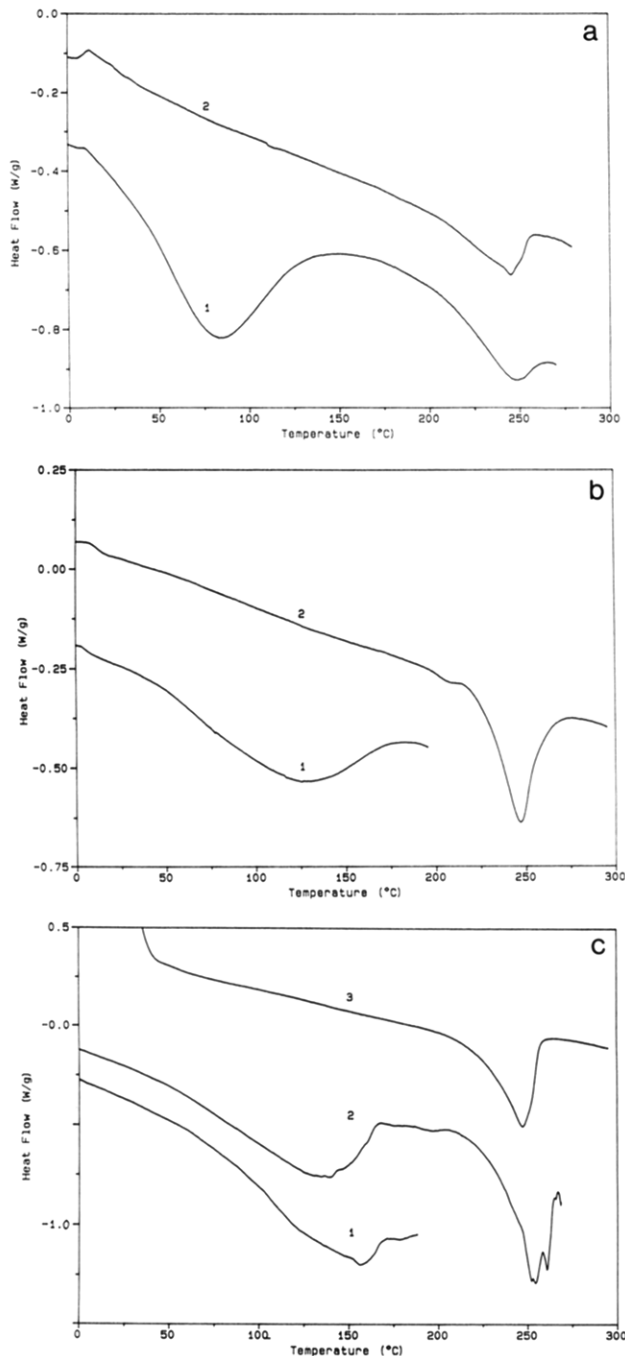


**Figure 6.** DSC thermograms of PBZT:nylon 66 molecular composites (a) 2:1, (b) 1:1, (c) 1:2. The curve numbers indicate the chronological order of DSC scans. Heating rate: 20 °C/min.

of the endotherm with increasing flexible-chain polymer content indicates an increasing thermal stability of composite morphology with increasing nylon 66 content. Since nylon 66 is highly crystalline, its  $T_g$  is not clearly visible in these composites but crystallization is evidenced by the reappearance of its melting point ( $T_m$ ) in all three composites.

On the other hand, PBZT/polyamide composites obtained by coagulation of the solid-state Lewis acid complexes are already phase separated as prepared. Figure 7 shows typical initial DSC thermograms of samples of such materials. Notably no broad endotherms are observed as were seen in Figures 5 and 6. Instead, transitions characteristic of the pure polyamides show up clearly in the first DSC heating scans. These results further support our interpretation of the endotherms in the first DSC

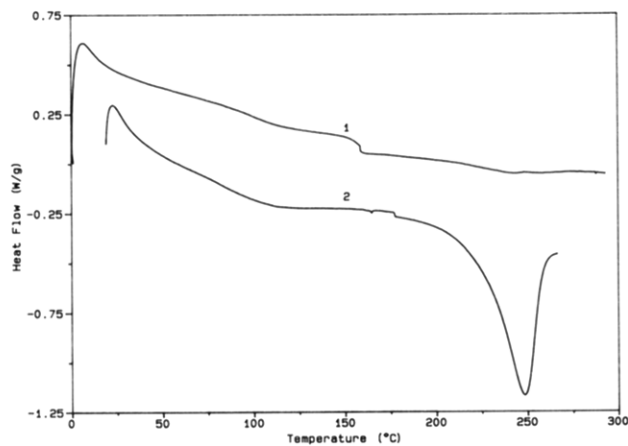
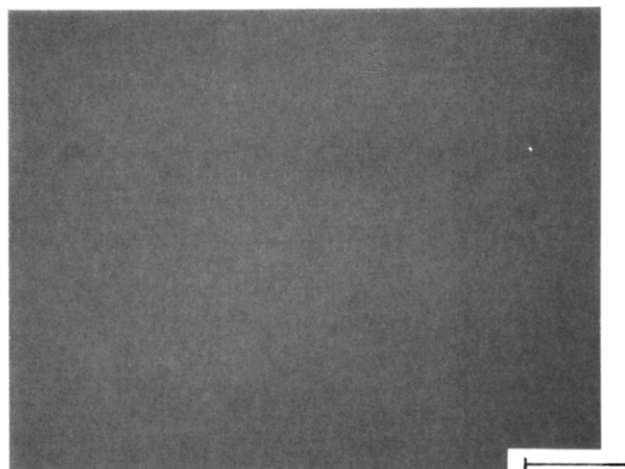
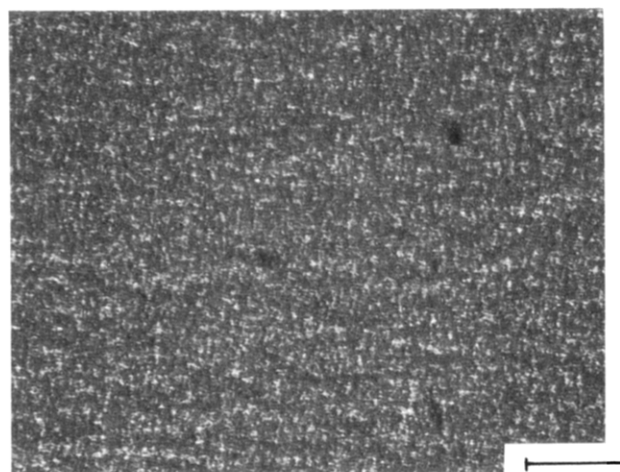


**Figure 7.** First scan DSC thermograms of (1) 1:1 PBZT:PTMHT and (2) 1:1 PBZT:nylon 66 coagulated from their solid  $\text{AlCl}_3$  complexes. Heating rate: 20 °C/min.



(a)

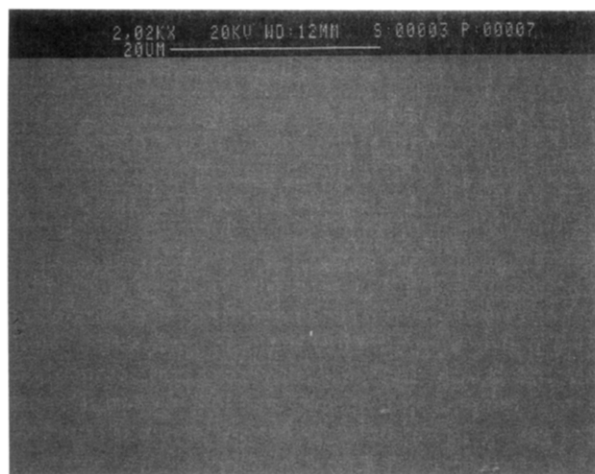


(b)

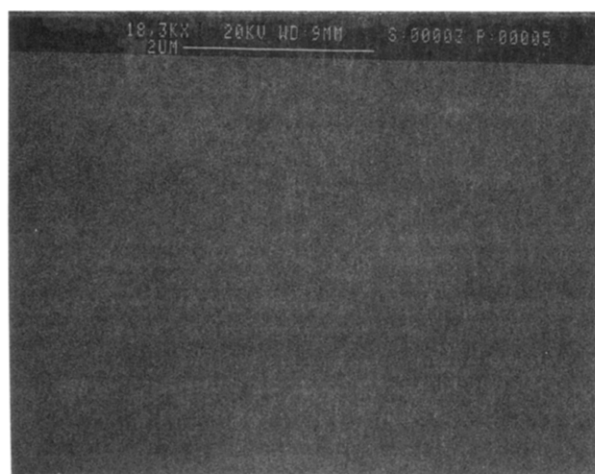
**Figure 8.** 1:1 PBZT:PTMHT film viewed between crossed polarizers at 1000 $\times$  (a) as processed from isotropic solution and (b) after heating to 250 °C.

heating scans observed in the PBZT/polyamide molecular composites of Figures 5 and 6 as thermally induced phase separation.

*Morphological Characterization.* Figure 8 shows optical micrographs of the 1:1 PBZT:PTMHT, as coagulated (a)



(a)

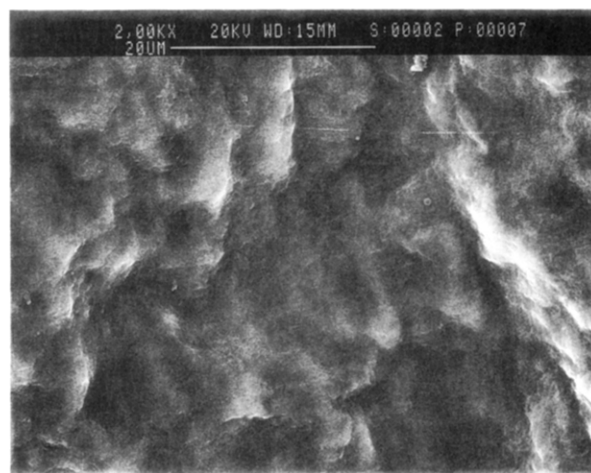


(b)

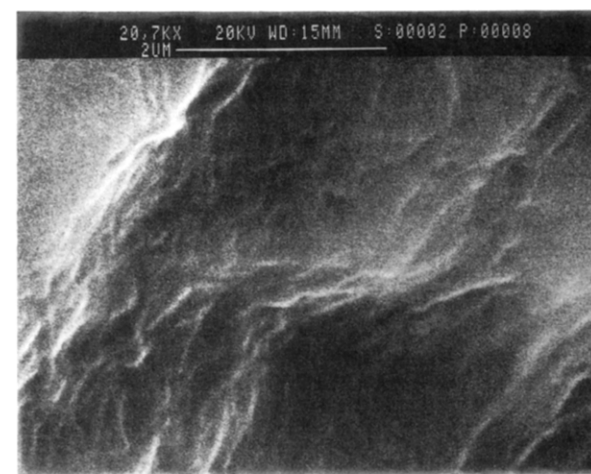
**Figure 9.** SEM micrographs of 1:2 PBZT:nylon 66 as processed from isotropic solution in  $\text{AlCl}_3/\text{NM}$  (a) 2020 $\times$ , (b) 18 300 $\times$ .

and after heating to 250  $^\circ\text{C}$  (b). This composition was chosen as representative of all the PBZT:PTMHT and PBZT:nylon 66 composites on which similar observations were made. The film of Figure 8a was coagulated from isotropic solution and was visually isotropic and transparent yellow. As is evident from the micrograph the composite exhibited no distinct morphological features at 1000 $\times$  indicating its uniformity to a level of better than 1  $\mu\text{m}$ . In sharp contrast, heating to 250  $^\circ\text{C}$  which is well above the  $T_g$  of PTMHT caused the sample to develop a distinctly phase separated morphology. Opaque white features appeared with dimensions of 1–3  $\mu\text{m}$  which, from their color, are most likely PTMHT rich. This was accompanied by visibly increased opaqueness and non-uniformity in the sample.

Figure 9 shows the SEM micrographs at two different magnifications of 1:2 PBZT:nylon 66 films. The sample is homogeneous at both magnifications. Energy dispersive X-ray analysis (EDAX) of the sample indicated a uniform sulfur profile at this magnification which implies a uniform dispersion of PBZT since nylon 66 contains no sulfur. The composite is therefore homogeneous to a level of 0.05–0.1  $\mu\text{m}$ . This sample is again representative of other composite compositions which were found to be similarly uniform.



(a)



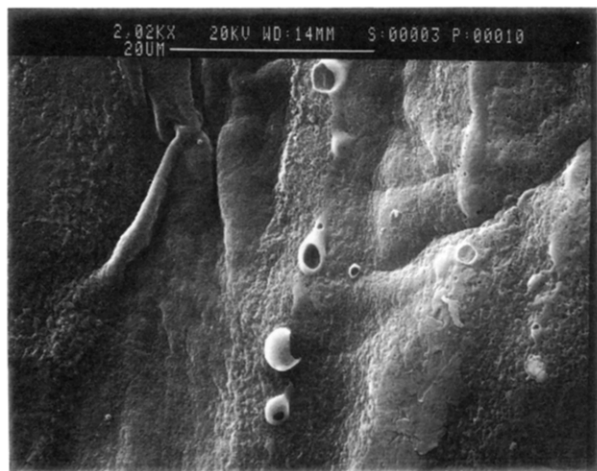
(b)

**Figure 10.** SEM micrographs of 1:2 PBZT:nylon 66 processed from isotropic solution in  $\text{AlCl}_3/\text{NM}$  followed by heating to 280  $^\circ\text{C}$  (a) 2000 $\times$  and (b) 20 700 $\times$ .

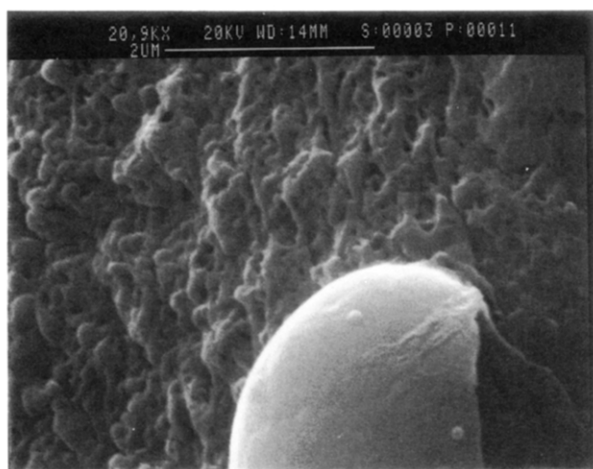
Figure 10 shows the morphology of a sample first prepared as was the sample of Figure 9 and subsequently heated to 280  $^\circ\text{C}$ , which is above the melting point of nylon 66. Regions of bright and dark contrast which are of micron dimensions are evident in Figure 10. Energy dispersive X-ray analysis showed that the areas of brighter contrast were PBZT rich due to their higher sulfur content than the darker areas. This shows that phase separation has been induced, as seen in the DSC and OM studies.

Figure 11 shows a 1:2 PBZT:nylon 66 sample which was coagulated from the solid  $\text{AlCl}_3$  complex of the composite. The bright craterlike features and brighter areas around them had higher PBZT content than the darker regions, which suggests aggregation of PBZT as seen in the sample of Figure 10. Along with the DSC studies of composites coagulated from their solid complexes (Figure 7) and studies of the  $T_g$  behavior of the complexes (Figure 3), these observations confirm the theoretical predictions<sup>21</sup> that coagulation under anisotropic conditions inevitably yields phase-separated materials. Since the complex samples were prepared by slow evaporation of solvent from isotropic solutions, at some point these solutions passed





(a)



(b)

**Figure 11.** SEM micrographs of 1:2 PBZT:nylon 66 processed from the solid  $\text{AlCl}_3$  complex (a) 2020 $\times$  and (b) 20 900 $\times$ .

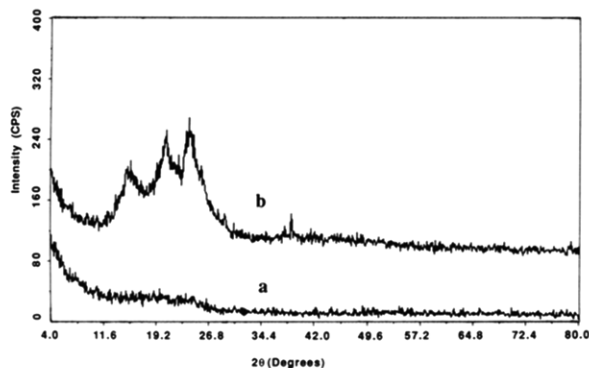


**Figure 12.** X-ray powder diffractograms of (a) as-prepared 1:2 PBZT:nylon 66 molecular composite; (b) 1:2 PBZT:nylon 66 film processed as in (a) and subsequently heated to 280 °C.

through the  $C_{cr}$  for that composition and the rigid-rod aggregated gradually in an anisotropic phase.

Figure 12a shows the X-ray powder diffractogram of an as-prepared 1:2 PBZT:nylon 66 molecular composite. No crystalline peaks were identified in this sample by computer data reduction. There is evidence of an amorphous halo in the approximate range 10–27°. Figure 12b shows the pattern for a similarly prepared sample which was

then heated to 280 °C. In this case there are crystalline peaks at  $2\theta$  values of 15.3, 20.7, and 24.0° corresponding to  $d$  spacings of 5.80, 4.29, and 3.71 Å, respectively. The diffraction pattern of Figure 12a is clear evidence for molecular dispersion of the rigid-rod polymer molecules in the flexible-chain polyamide matrix. Any aggregates of the PBZT formed can consist of no more than a few of rigid-rod molecules since no diffraction maxima are observed. Furthermore the absence of any nylon 66 diffraction peaks indicates the complete disruption of the crystalline polyamide matrix by the PBZT molecules as would be the case with molecular dispersion.

However, the crystalline peaks in Figure 12b show that phase separation due to heating at 280 °C has taken place. Studies of the crystal structure of PBZT have been carried out by others<sup>33,34</sup> which revealed lateral spacings of 5.85 and 3.54 Å, the (100) and (010) reflections, respectively. Our studies of nylon 66 coagulated from Lewis acid complex solutions revealed peaks at 24.1° and 20.5° corresponding to  $d$  spacings of 3.68 and 4.33 Å, respectively, and indicative of the  $\alpha$ -crystalline form.<sup>35</sup> The peaks in Figure 12b can thus be assigned as follows: The 5.80-Å peak is the (100) reflection of PBZT. The 4.29-Å peak is the nylon 66 (100) reflection, and the 3.71-Å peak is a combination of the (010) reflections of PBZT and nylon 66. Assuming that peak broadening arises solely from crystallite sizes, the crystallite dimensions can be estimated using the Scherrer formula:<sup>36</sup>

$$L = K\lambda/\beta \cos \theta$$

$L$  is the lateral coherence length,  $K$  is a constant usually taken to be unity,  $\beta$  is the full width at half-maximum of the reflection, and  $\lambda$  and  $\theta$  have their usual meaning for X-ray diffraction. Approximate estimates of  $L$  for the 5.80-, 4.29-, and 3.71-Å reflections are 1.59, 1.75 and 2.34 nm, respectively. Cross sections of PBZT crystallites are therefore on the order of 1.6 nm  $\times$  2.3 nm. Presumably aggregates of these crystallites account for the PBZT rich regions seen in the SEM photos of these phase separated composites such as in Figures 10 and 11. This is in direct contrast to the molecularly dispersed composite of Figure 12a where the lateral dimensions of any aggregates are at most a few angstroms.

Figures 13 and 14 show FTIR spectra of the as-processed PBZT/polyamide molecular composites. In all cases the spectra are exact superimpositions of the spectra of the component polymers. That is, there are no apparent shifts in the bands of either polymer in any composite. The trend of increasing intensity of the PBZT bands (most notably the strong 1484- and 959- $\text{cm}^{-1}$  bands) relative to the intensities of the polyamide bands (e.g., the N-H stretches at 3300  $\text{cm}^{-1}$  and the carbonyl stretches at 1640  $\text{cm}^{-1}$ ) with increasing weight percent of PBZT in the composites is evidence of composite homogeneity and composition. The fact that there are negligible shifts in the vibrational bands of either polymer in both types of composite (PBZT/nylon 66 and PBZT/PTMHT) seems to indicate the absence of any strong interpolymer attractive forces such as hydrogen bonding between PBZT and polyamide or repulsive forces. This provides some

(33) Roche, E. J.; Takahashi, T.; Thomas, E. L. *Am. Chem. Soc. Symp. Ser. Diffraction Methods* 1980, 141, 303-313.

(34) Allen, S. R.; Farris, R. J.; Thomas, E. L. *J. Mater. Sci.* 1985, 20, 4583-4592.

(35) Roberts, M. F.; Jenekhe, S. A. Submitted to *Macromolecules*.

(36) Kakudo, M.; Kasai, N. *X-Ray Diffraction by Polymers*; Elsevier: New York, 1972; p 329.

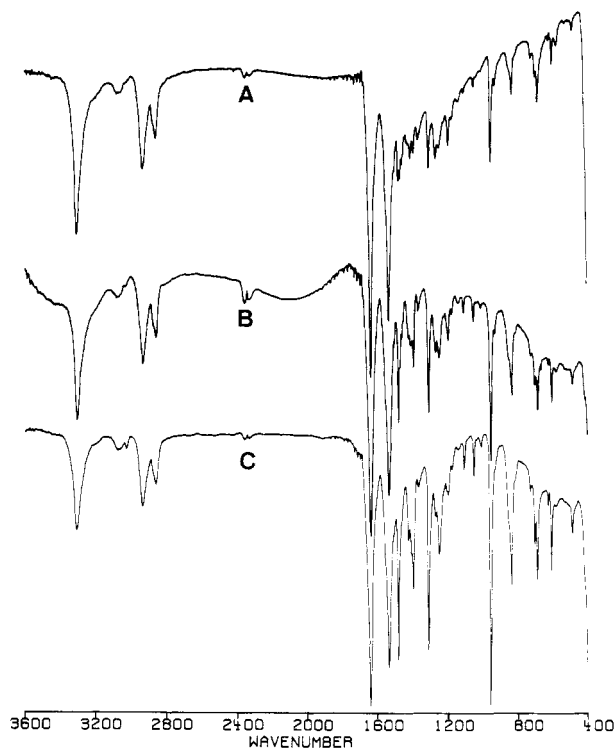


**Figure 13.** FTIR spectra of PBZT:nylon 66 molecular composites (a) 1:2, (b) 1:1, and (c) 2:1.

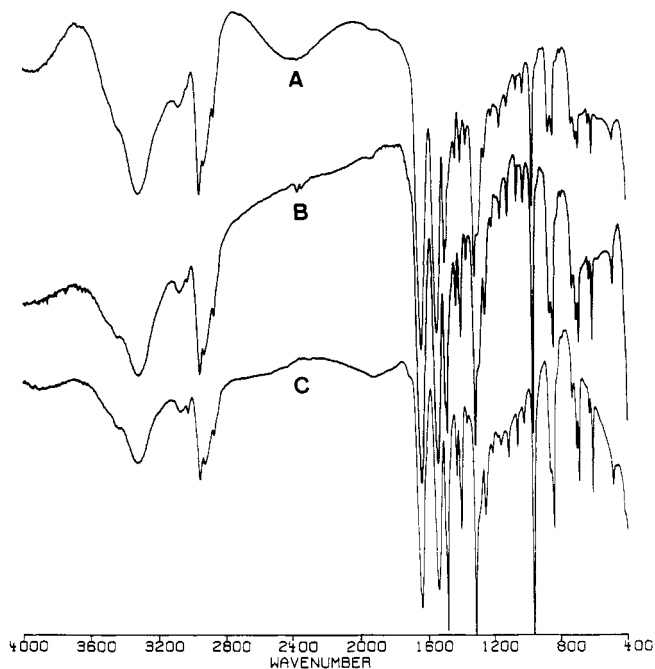


**Figure 14.** FTIR spectra of PBZT:PTMHT molecular composites (a) 1:2, (b) 1:1, and (c) 2:1.

insight into the causes for thermal instability of the molecular composite morphology discussed earlier. As pointed out by Flory,<sup>21</sup> entropic forces which arise from configurational differences between rod and coil polymers, favor phase segregation to minimize free energy. Therefore unless there are sufficient retarding forces such as strong intermolecular attractions, the input of thermal energy will allow the rod/coil system which has been frozen into the metastable state of molecular dispersion by rapid coagulation, to phase separate. The sluggishness of molecular motions in PBZT, nylon 66 and PTMHT below

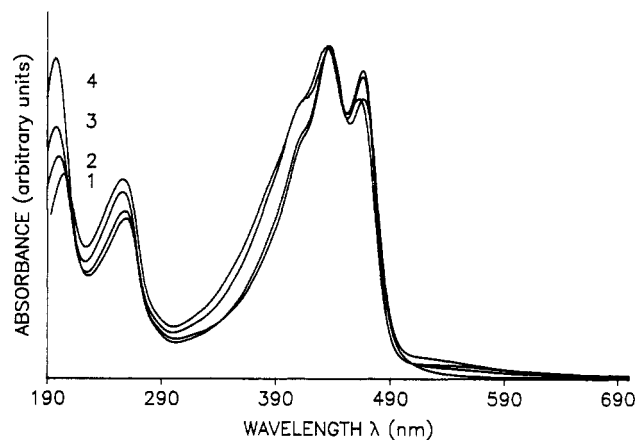


**Figure 15.** Electronic absorption spectra of molecular composites of PBZT:nylon 66 (1) 1:0, (2) 2:1, (3) 1:1, and (4) 1:2.

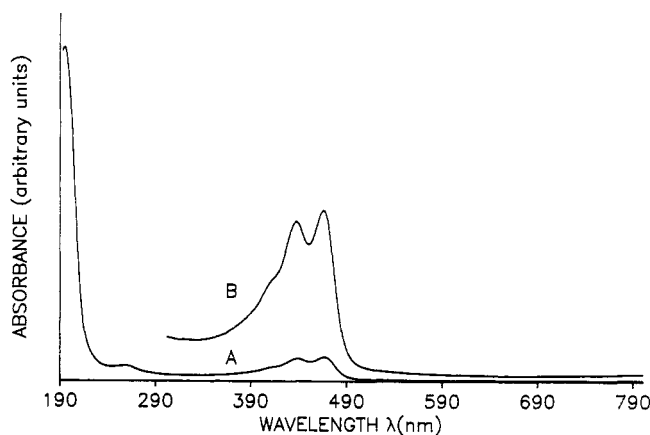


**Figure 16.** The electronic absorption spectrum of 1:100 PBZT:nylon 66 molecular composite (A). Spectrum B shows an enlargement of spectrum A in the region 300–800 nm.

their  $T_g$ 's or  $T_m$ 's are sufficient to prevent this from happening at room temperature.

The electronic absorption spectra of PBZT/nylon 66 composites are presented in Figure 15 along with the spectrum of PBZT. The spectra were all normalized to coincide at the 435-nm peak for comparison purposes, since this peak in the main absorption band of PBZT appeared prominently in all spectra. From the figure it is clear that as the polyamide content in the composites increases, there is a gradual increase in the relative intensity of the amide group transition at 200 nm. Concurrently there is a gradual narrowing of the main absorption band of PBZT. Full width at half-maximum (fwhm) values of 1:0, 2:1, 1:1, and 1:2 PBZT:nylon 66 are 106, 100, 85, and 81 nm, respectively. This bandwidth narrowing arises from a monotonic decrease in intermolecular electronic interactions in PBZT with increasing molecular dispersion of the rigid rod polymer in the matrix of the nonconjugated aliphatic polyamide. The optical absorption spectrum of 1:100 PBZT:nylon 66 is given in Figure 16. In this case increased molecular dispersion of PBZT yields a fwhm value of 77 nm. PBZT dissolved at a concentration of  $10^{-4}$  M in  $AlCl_3/NM$  has a fwhm of 61 nm which, neglecting the effects of solvation, can be thought of as representing very highly dispersed rods in a nonconjugated matrix. Thus the trend of fwhm supports the notion of dispersion of rod molecules in a flexible coil matrix in a molecular composite. We also induced phase separation in each composite of Figures 15 and 16 by heating to 280 °C. This resulted in a broadening

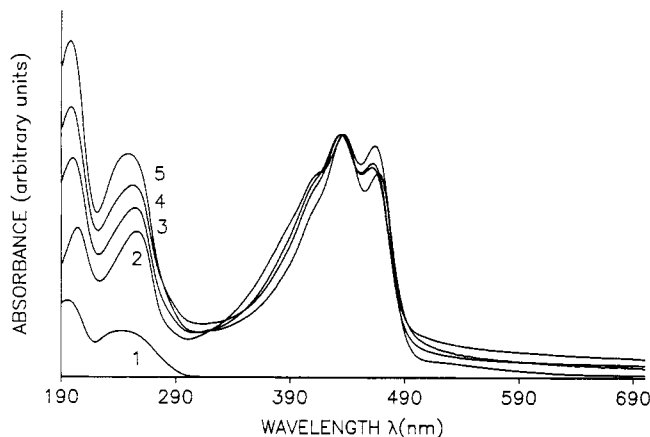


**Figure 17.** Electronic absorption spectra of molecular composites of PBZT:PTMHT (1) 0:1, (2) 1:0, (3) 2:1, (4) 1:1, and (5) 1:2.

of the PBZT main band in all cases, consistent with aggregation of PBZT in the samples.

Figure 17 shows the absorption spectra of PBZT/PTMHT composites and of PBZT and PTMHT, normalized at 435 nm as for the PBZT/nylon 66 composites. The increasing intensity of the 200 nm amide transition is evident with increasing PTMHT content. There is also a monotonic increase in the 255 nm  $\pi-\pi^*$  transition of the aromatic ring of PTMHT. The band narrowing observed in Figure 15 is also apparent in the PBZT/PTMHT molecular composites. FWHM values of the PBZT main absorption band of 2:1, 1:1, and 1:2 PBZT:PTMHT are 97, 92, and 86 nm, respectively. Thus band narrowing of the PBZT  $\pi-\pi^*$  transition in the PBZT/PTMHT composites also provides evidence of molecular dispersion in the materials.

### Concluding Remarks

A new approach to the preparation of molecular composites of rigid-rod and flexible-chain polymers is

reported. Coordination complexes of rigid-rod PBZT and flexible-chain polyamides, nylon 66, and PTMHT with Lewis acids  $AlCl_3$  and  $GaCl_3$  were prepared in organic solvents. Solubilization of both rod and coil polymers in nitromethane affords high critical concentrations and facile processing of molecular composites from isotropic solutions by rapid coagulation in a nonsolvent. Morphological studies by visual observation, OM, DSC, SEM, and wide-angle X-ray diffraction show that the as-prepared PBZT/polyamide composites, processed from isotropic solutions of their Lewis acid complexes, are uniform at all magnifications, from the bulk scale down to the molecular level. They can therefore be called true molecular composites according to the definitions given in the introduction. The effects of molecular dispersion of the PBZT in the nonconjugated polyamide matrices are apparent in the electronic absorption spectra where decreased intermolecular interactions between increasingly dispersed PBZT molecules leads to a narrowing of its main absorption band. Thermally induced phase separation in these composites occurs at high temperatures as evidenced by morphological studies (OM, DSC, SEM, and wide-angle X-ray diffraction). Thermal instability of the heated molecular composite morphology is attributed to entropic driving forces and the absence of stabilizing interpolymer attractive forces. The proposed complexation-mediated processing of molecular composites which has been demonstrated here with PBZT/polyamides is applicable to many other heterochain rigid-rod/flexible-chain polymer systems.

**Acknowledgment.** This research was supported in part by the Amoco Foundation, the National Science Foundation (CTS-9311741), the NSF Center for Photo-induced Charge Transfer (Grant CHE 912-0001), and an Elon Huntington Hooker Fellowship to M.F.R. We thank the Polymer Branch of the Air Force Materials Laboratory, Dayton, OH, for a PBZT sample.